Circular Permutation and Deletion Studies of Myoglobin Indicate that the Correct Position of Its N-Terminus Is Required for Native Stability and Solubility but Not for Native-like Heme Binding and Folding†

Euripedes A. Ribeiro, Jr. and Carlos H. I. Ramos*

Centro de Biologia Molecular Estrutural, Laboratório Nacional de Luz Síncrotron, P.O. Box 6192, Campinas SP, 13084-971 Brazil, and Departamento de Bioquímica, Instituto de Biologia, Universidade Estadual de Campinas, Campinas SP, Brazil

Received September 27, 2004; Revised Manuscript Received December 6, 2004

ABSTRACT: We studied the effect of deleted and circularly permuted mutations in sperm whale myoglobin and present here results on three classes of mutants: (i) a deletion mutant, Mb_{1-99}, in which the C-terminal helices, G and H, were removed; (ii) two circular permutations, Mb-B_GHA, in which helix B is N-terminal and helix A is C-terminal, and Mb-C_GHAB, in which helix C is N-terminal and helices A and B are C-terminal; and (iii) a deleted circular permutation, Mb-HAB_F, in which helix H is N-terminal, helix F is C-terminal, and helix G is deleted. The conformational characteristics of the apo and holo forms of these mutants were determined at neutral pH, by spectroscopic and hydrodynamic methods. The apo form of the deleted and permuted mutants exhibited a stronger tendency to aggregate and had lower ellipticity than the wild type. The mutants retained the ability to bind heme, but only the circularly permuted holoproteins had native-like heme binding and folding. These results agree with the theory that myoglobin has a central core that is able to bind heme, but also indicate that the presence of N- and C-terminal helices is necessary for native-like heme pocket formation. Because the holopermuteins were less stable than the wild-type protein and aggregated, we propose that the native position of the N-terminus is important for the precise structural architecture of myoglobin.

In the hierarchy of protein structure, strands and helices are the basic building blocks that assemble to form the protein topology (*1*, *2*). Therefore, techniques such as serial deletions and circular permutations of these blocks permit the investigation of the architecture of proteins and are of special interest because the results add to the general understanding of protein folding and stability (*3*−*6*). Serial deletion approaches allow the identification of protein regions involved with function, folding, or both, and circular permutation approaches allow the study of topological changes in the protein, helping to identify folding elements in its structure. The circular permutant can be visualized as a polymer that has its N- and C-termini linked and then exposed to cleavage in another site, to create new termini (*7*). The importance of deletion and permutation approaches is shown by the large number of specific works that have used these protein engineering methods to produce insightful results on protein structure and function: functionality of BPTI circular permutations (*7*), enzymatic reactions of circularly permuted mutants of PRA isomerase (*8*), structure and stability of T4 lisozyme (*9*), folding of serial deletion mutants of CI2 (*10*), folding pathway of circular permutations of the α-spectrin SH3 domain (*11*), identification of functional regions of TnI (*12*), and combined deletion and circular permutation studies of protein stability and structure of dihydrofolate reductase (*13*). The permutants very often fold into a stable and functional structure, leading to the hypothesis that the correct position of the N-terminus is not required for proper folding (*4*). These results are somehow surprising considering the Anfinsen hypothesis (*14*), which states that the amino acid sequence determines the three-dimensional structure of a protein. It is, therefore, important to analyze the effect of such changes in model proteins to test the generality of this approach, and to collect data that add to our general understanding of protein folding and stability.

Myoglobin (Mb)[1] is an archetype of the globin family and has been widely studied from functioning to folding (see refs *15*−*18* and references therein). Mb is monomeric and is formed by eight α-helices that are named A−H (*19*) (Figure 1A). NMR studies (*20*−*22*) showed that apoMb, Mb without the heme group, is structurally similar to holoMb, except for an unfolded F helix. Under mildly acid conditions, apoMb forms an intermediate in which its N- and C-terminal helices

† This work was funded by Fundação de Amparo a Pesquisa do Estado de São Paulo, Conselho Nacional de Pesquisa e Desenvolvimento, and PEW Charitable Trusts. E.A.R. holds a FAPESP fellowship.

* To whom correspondence should be addressed. E-mail: cramos@lnls.br. Phone: 55-19-3512-1118. Fax: 55-19-3512-1006.

[1] Abbreviations: Mb, myoglobin; WT, wild type; Mb_{1-123}, Mb with residues 124−153 deleted (helix H); Mb_{1-99}, Mb with residues 100−153 deleted (helices G and H); Mb-C_GHAB, circularly permuted protein that starts at residue S35 (using WT residue numbering) and ends at residue K34; Mb-B_GHA, circularly permuted protein that starts at residue A19 and ends at residue E18; Mb-HAB_F, circularly permuted and deleted protein that starts at residue G124 and ends at residue I99; SDS−PAGE, sodium dodecyl sulfate−polyacrylamide gel electrophoresis; T_m, temperature at the midpoint of the thermal transition; *A*, absorbance; CD, circular dichroism; AUC, analytical ultracentrifugation; NMR, nuclear magnetic resonance; Bis-ANS, bis-1-anilino-8-naphthalenesulfonate.

10.1021/bi047908c CCC: $30.25
Published on Web 03/05/2005

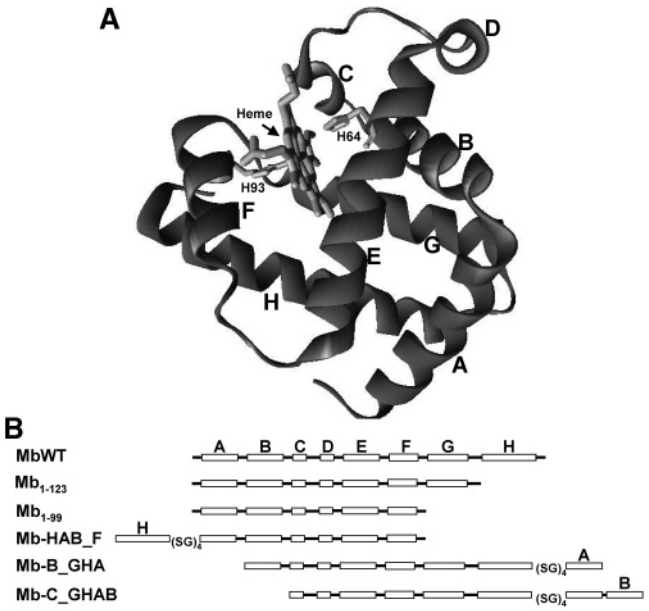

FIGURE 1: (A) Three-dimensional structure of sperm whale Mb. The Mb (PDB entry 5MBN) diagram was created using WebLab ViewerLite version 3.7 (Molecular Simulations Inc.). Helices are named A−H. The heme and the histidine residues involved in its coordination are identified. (B) Schematic representation of the α-helix positions in WT, deleted, and circularly permuted Mb. The permutein Mb-HAB_F has helix G deleted and has helix H in its N-terminus and helix F in its C-terminus, starting at residue G124 and ending at residue I99. The permutein Mb-B_GHA has helix B in its N-terminus and helix A in its C-terminus, starting at residue A19 and ending at residue E18. The permutein Mb-C_GHAB has helix C in its N-terminus and helices A and B in its C-terminus, starting at residue S35 and ending at residue K34. $(SG)_4$ represents the SGSGSGSG linker.

remain partially folded (*15*, *18*). This intermediate is formed by helices A, G, and H as shown by both equilibrium (*23*) and kinetic studies (*24*). Jennings and Wright (*22*) showed that the last residues of helix B are also protected in the intermediate, suggesting that this helix is partially incorporated into the intermediate domain during folding, with the remainder being incorporated later (*25*). B helix sequential folding is supported by hydrogen exchange (*26*), site-directed mutagenesis (*27*), and NMR (*21*) experiments. Together, these works suggest that the A[B]GH domain is the core of the apoMb intermediate. However, the extent of B helix folding in the intermediate is still unknown, and although the formation of the A[B]GH domain in the intermediate is considered to be an important step for apoMb to reach its native state (*15*, *18*), folding experiments with Mb fragments, which lack varied portions of the A[B]GH core, suggest that this theory could be inaccurate. Deletion studies in which both N- and C-termini of apoMb were deleted showed that a minimum core, formed by residues 29−105, is fairly folded and capable of binding heme (*28*). The Mb fragment of residues 29−105 achieves a far-UV CD spectrum shape, similar to that of the WT Mb spectrum in its native state, only when heme is bound, suggesting that the Mb heme-binding subdomain is dependent on the cofactor (heme) (*28*). More surprisingly, a fragment comprising residues 32−139, which lacks helices A and B and part of helix H, is also capable of forming an intermediate under mildly acid conditions, challenging the theory that these helices form the intermediate (*29*).

ApoMb mutants deleted from C-terminal helices are mostly unfolded (*30*, *31*), form aggregates (*30*), and experienced severe decreases in their heme binding capacity (*31*). Although deletions seem to cause a partial structure loss in apoMb, a circular permutation, where helix H is N-terminal and helix G is C-terminal, seems to result in a protein with native-like folding (*32*). We believe that a more comprehensive understanding of the role of helices A, B, G, and H for the folding and stability of the holo and apo forms of Mb can emerge from a detailed investigation of specific deletions and permutations of these helices. These mutants can also help in investigating whether the native N-terminus is a requirement for the proper folding of Mb. Therefore, we made a series of deleted and circularly permuted mutants of Mb and produced three classes of mutants: (i) a deletion mutant, Mb_{1-99}, in which helices G and H were removed; (ii) two N-terminal circular permutants, Mb-B_GHA, in which helix B is N-terminal and helix A is C-terminal, and Mb-C_GHAB, in which helix C is N-terminal and helices A and B are C-terminal; and (iii) a deleted circular permutant, Mb-HAB_F, in which helix H is N-terminal, helix G is deleted, and helix F is C-terminal (Figure 1B). In this work, to further comprehend the role of the N- and C-terminal helices in native stability and heme pocket formation of Mb, we studied the conformational characteristics of the apo and holo forms of these mutants by spectroscopic and hydrodynamic methods, at neutral pH, and compared them with previous results of deleted and permuted Mb mutants in the literature (*28*−*32*). Our results indicated that although Mb has a central core that is capable of binding heme, the presence of helices A, B, G, and H is necessary for native folding and for native-like heme pocket formation. And, since the circular permutations had low stability and a strong tendency to aggregate, we propose that the position of the N- and C-termini of Mb has to be native-like for the precise structural architecture of this protein.

EXPERIMENTAL PROCEDURES

Construction of the Template Vectors. The pT7-7-Mb vector, in which sperm whale Mb cDNA is cloned (*31*), was used as a template to construct the pT7-7-2Mb vector using a two-step PCR-based site-directed mutagenesis approach. For the first PCR, the standard sperm whale Mb cDNA forward primer 5′AGGAGAACAACACATATGGTTCTGTCTGAA3′, which contains an *Nde*I restriction site and an initiation codon, and the 2Mb reverse primer 5′ACCAGAACCGGAGCCAGATCCGCTACCCTG3′, which removes the stop codon and adds codons for a link of residues (SGSGS) and for the *Bsa*WI restriction site, were used. For the second PCR, the 2Mb forward primer 5′TCTGGCTCCGGTTCTGGTATGGTTCTG3′, which adds the *Bsa*WI restriction site and the codons for residues GSG followed by the first methionine residue, was used with the standard sperm whale Mb cDNA reverse primer 5′TGCAGGTCGACCCCCCGG3′. The PCR products were digested with *Bsa*WI and ligated. This procedure resulted in a DNA sequence with two Mb cDNA (2Mb) cloned in tandem and in frame by a nucleotide sequence encoding an SGSGSGSG [$(SG)_4$] linker. The 2Mb cDNA was double-digested with *Nde*I and *Sal*I and subcloned into a pT7-7 vector digested with the same enzymes. This procedure created the pT7-7-2Mb vector, which was confirmed by DNA sequencing.

Construction of the Deleted and Circularly Permuted Mutants. The forward primer 5′AGGAGAACAACACATATGGTTCTGTCTGAA3′ was used with the reverse primer 5′TCGCATGCTACTAAACATAAGATTTAAATCAAATACCTG3′ for the construction of the mutant Mb_{1-99}, deleted from helices G and H, using pT7-7-Mb as a template, as described for deleted mutant Mb_{1-123} (*31*). The pT7-7-2Mb vector was used as a template to create the circularly permuted Mbs by PCR. Each forward oligo was designed to anneal to the first Mb sequence of the 2Mb cDNA, in the region covering the requested codon for the first residue in the permutein, inserting a site for the restriction enzyme *Nde*I and the start codon for methionine. Each correlate reverse primer was designed to anneal to the second Mb sequence of the 2Mb cDNA, in the region covering the requested codon for the last residue in the permutein, creating a stop codon and inserting an upstream site for the *Bam*HI restriction enzyme. The PCR product was then double-digested with *Nde*I and *Bam*HI, and the fragment was cloned into a pET3a vector (Novagen) for heterologous expression. This strategy was used to create the permuteins cDNAs: Mb-C_GHAB, by using the forward primer 5′TTGATTCGACTGCATATGTCTCATCCGGAA3′ and the reverse primer 5′CAGAGGATCCGGATGTTATTTGAACAGTC3′; Mb-B_GHA, by using the forward primer 5′GTTTGGGCTAAACATATGGCTGACGTCGCT3′ and the reverse primer 5′ATGACCAGGGATCCTTATTCAACTTTAGCC3′; and Mb-HAB_F, by using the forward primer 5′CAGGTGACCATATGGCTGACGCTC3′ and the reverse primer 5′AATTCCAGGATCCGATTTAGATCTTATGT3′. The constructs were confirmed by DNA sequencing.

Protein Expression and Purification. The expression and purification of WT and mutants were performed with a method previously described (*31*), in which the protein is purified directly in its apo form. Protein expression at 37 °C was also tested to monitor the reddish brown color of the bacterial pellet, an indication of in vivo heme binding. The purification procedure was followed by the chromatographic step for removal of nucleic acid contamination to certify that the $A_{280/260}$ ratio was higher than 1.5 (*33*). After purification, the proteins were exhaustively dialyzed against water, lyophilized, and stored at −80 °C. The purity of the proteins was evaluated by SDS−PAGE, and the apoMb concentration was determined spectrophotometrically as previously described (*34*, *35*). The holoMb was prepared by adding hemin to the protein in 50 mM sodium phosphate buffer (pH 6.0), and cyanoholoMb was prepared from holoMb by adding KCN (*36*) followed by a gel filtration chromatography step to eliminate unbound forms. The formation of oxidized and cyanide holoMb was monitored by absorbance at the Soret band, and the holoMb concentration was calculated as previously described (*37*). A cyanoMb preparation was used if its concentrations calculated at A_{280} ($\epsilon_{280} = 35.0\ mM^{-1}\ cm^{-1}$) and A_{423} ($\epsilon_{280} = 109.7\ mM^{-1}\ cm^{-1}$) varied by less than 10%. Mass spectrometry measurements for molecular mass determination and Edman degradation chemistry for N-terminal amino acid sequencing were performed at the Mass Spectrometry Facility at UNICAMP. All chemicals were analytical grade.

Gel Filtration Chromatography. The homogeneity of the Mb apo and holo forms was checked by gel filtration chromatography. Gel filtration chromatography was carried out with a Superdex 75 HR 10/30 column coupled to an HPLC system (Amersham Pharmacia, Uppsala, Sweden). The column was equilibrated with at least 2 column volumes of the appropriate buffers at a flow rate of 0.5 mL/min, and each protein (0.5−1.5 mg/mL) was applied to the column and eluted with 50 mM sodium phosphate (pH 7.0) and 150 mM NaCl. The elution profiles were determined by the absorbance at wavelengths of 280 and 423 nm. The apparent molecular masses were estimated by comparison with the elution profile of standard proteins: chicken egg white lysozyme (14 300 Da), bovine pancreas ribonuclease A I (16 500 Da), horse heart Mb (16 950 Da), and bovine serum albumin (67 000 Da).

Circular Dichroism Measurements. A JASCO model J-810 CD spectropolarimeter equipped with a thermoelectric sample temperature controller (Peltier system) was used to record the CD spectra. The data were collected from 260 to 200 nm for spectral measurements and at 222 nm for stability measurements. The CD spectra were accumulated 10 times. All measurements were taken in cuvettes with a path length of 1 cm and with a protein concentration of 1 μM at 50 mM sodium phosphate (pH 6.0) and 0.5 mM KCN. The α-helix content was also determined using the recorded data at 222 nm (*38*). The heat-induced unfolding and refolding were recorded at 222 nm, every 1 °C, at a scan rate of 40 °C/h. The average of at least three unfolding experiments was used to build each curve profile, and the T_m is the temperature at the midpoint of the unfolding transition. Curve fitting was carried out using Origin (Microcal).

Fluorescence Measurements. Fluorescence measurements were recorded in an Aminco Bowman Series 2 (SLM-AMINCO) luminescence spectrometer. The emission fluorescence spectra of tryptophan were measured with an apoMb concentration of 1 μM with excitation at 280 nm (band-pass of 4 nm), and emission was measured from 300 to 450 nm (band-pass of 16 nm). HoloMb at a concentration of 2 μM and bis-ANS at concentrations of 1.0−3.0 μM were incubated for 20 min at 20 °C, and the emission fluorescence spectra were recorded with excitation at 365 nm (band-pass of 4 nm); emission was measured from 400 to 600 nm (band-pass of 8 nm). The intrinsic emission fluorescence data were analyzed either by their emission maxima wavelength or by their spectral center of mass ($\langle\lambda\rangle$) as described by the equation

$$\langle\lambda\rangle = \sum\lambda_i F_i / \sum F_i \qquad (1)$$

where λ_i is each wavelength and F_i is the fluorescence intensity at λ_i. All data were analyzed with Origin (Microcal).

Analytical Ultracentrifugation. Sedimentation velocity experiments were performed with a Beckman Optima XL-A analytical ultracentrifuge. The WT, Mb-C_GHAB, and Mb-B_GHA proteins were tested at concentrations from 1.5 to 6.0 μM in 50 mM sodium phosphate buffer (pH 6.0), 50 mM NaCl, and 0.5 mM KCN. The sedimentation velocity experiments were carried out at 20 °C and 40 000 rpm (AN-60Ti rotor), and the scan data were acquired at 423 nm. All fittings were performed using either Origin (Microcal Software) supplied with the instrument or Sedfit (39). The van Holde−Weischet (sediment coefficient plot) (*40*), Second Moment (*41*), Transport (*42*), and Sedimentation Time Derivative [$g(s^*)$ integral distribution] (*43*) methods were used to analyze the experiments. The methods used for

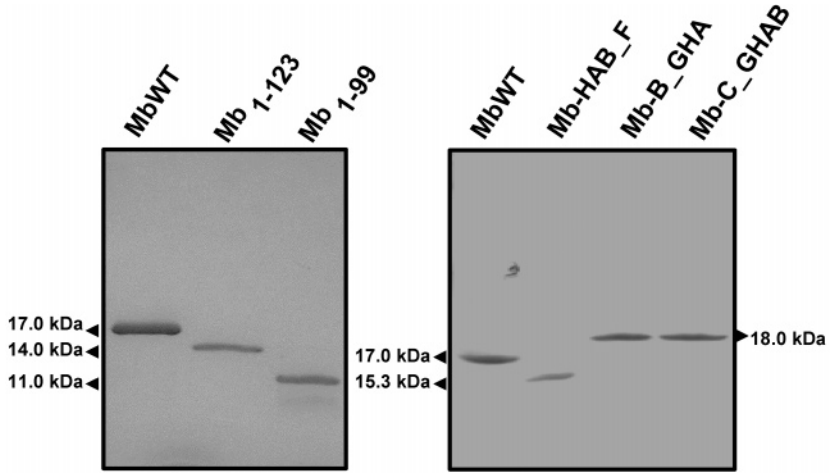

FIGURE 2: Purified WT, deleted, and circularly permuted myoglobins. SDS−PAGE shows that the proteins were purified with the expected relative molecular mass.

analyzing the velocity experiments allowed the calculation of the apparent sedimentation coefficient *s*, the diffusion coefficient *D*, and the molecular mass *M*. The ratio of the sedimentation to diffusion coefficient gave the molecular mass:

$$M = \frac{sRT}{D(1 - V_{bar}\rho)} \quad (2)$$

where *R* is the gas constant, *T* is the absolute temperature, V_{bar} is the protein partial specific volume, and ρ is the buffer density. The Sednterp software (www.jphilo.mailway.com/download.htm) was used to estimate the protein's partial specific volume at 20 °C (V_{bar}WT = 0.750 mL/g, V_{bar}Mb-C_GHAB = 0.746 mL/g, and V_{bar}Mb-B_GHA = 0.746 mL/g), buffer density (ρ = 1.00734 g/mL), and buffer viscosity ($\eta = 1.002 \times 10^{-2}$ P). These values were used in the following equation (*44*):

$$s_{sphere} = 0.012 \frac{M^{2/3}(1 - V_{bar}\rho)}{V_{bar}^{1/3}} \quad (3)$$

that predicts the sedimentation velocity coefficient values for a protein with mass *M* and partial specific volume V_{bar}, which has a smooth compact spherical shape. The predicted values were then compared with the measured values to evaluate the shape and the compactness of the WT and permutant proteins in water.

RESULTS

Production of Mutants. A genetic engineering approach was used to create a DNA sequence composed of two sperm whale Mb cDNAs linked by a sequence of serine and glycine residues [$(SG)_4$ linker]. The sequence of the linker was chosen because it works as a hinge with low probability of having secondary structure, which could compromise the folding of the two adjacent helices, A and H, and has a size that does not interfere with the global structure of the engineered protein (*32*). The 2Mb cDNA permits the construction of a diverse variety of Mb permutants with a linker between helices A and H (Figure 1B). The deleted and circularly permuted mutants were expressed in large quantities in the inclusion body fraction even at 37 °C, and the bacterial pellets were not reddish brown. The proteins were highly pure (Figure 2), and had lower yields than the WT (6 mg/mL for Mb-HAB_F, 10 mg/L for Mb-C_GHAB, 20 mg/L for either Mb-B_GHA or Mb_{1-99}, and 40 mg/mL for WT apoMb). The correct identities of the proteins were confirmed by mass spectrometry and Edman degradation experiments (data not shown).

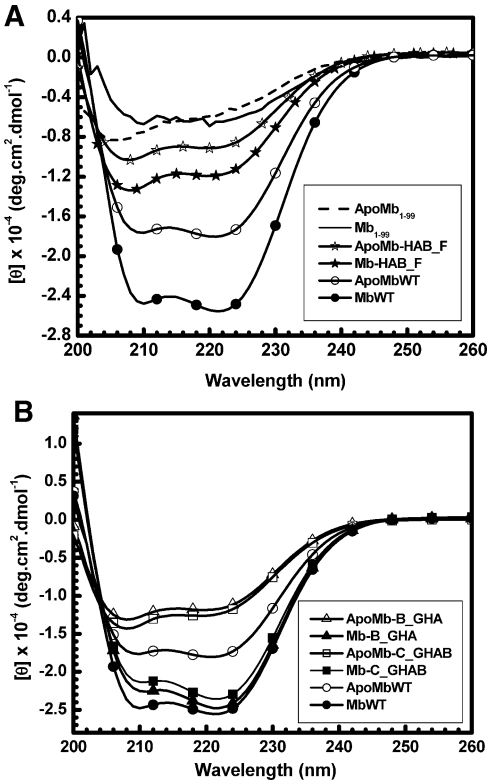

FIGURE 3: Far-UV CD spectra of the apo and holo forms of Mb. Far-UV CD spectra from 200 to 260 nm are shown for WT and mutants at pH 6.0. (A) WT and deleted mutants. Apo and holo forms of the deleted mutants have CD profiles characteristic of partially folded proteins, with much lower ellipticities and α-helical contents than the WT (see also Table 1). (B) WT and circularly permuted mutants. The holo permuteins have native-like CD profiles. However, the apo permuteins have much lower ellipticities and α-helical contents than WT apoMb (see also Table 1).

The Apo Forms of the Deleted and Circularly Permuted Mutants Were Less Structured than WT. The CD spectrum profile of the deleted (Figure 3A) and permuted (Figure 3B) mutants, in the apo form, were characteristic of proteins with secondary structure formed by α-helices, but with lower

Table 1: Spectroscopic Parameters for Apo and Holo Forms of WT and Mutant Mbs[a]

protein	CD_{222} (deg cm^2 dmol^{-1})	α-helix (%)	center of mass $\langle\lambda\rangle$ (nm)[b]	Soret band λ_{max} (nm)[c]	A_{423}/A_{280}	Bis-ANS binding
apo WT	−18000	65	338	–	–	–
WT Mb	−25000	85	–	422 (408)	3.2	no
apoMb$_{1-123}$[d]	−2800	20	345	–	–	–
apoMb$_{1-99}$	−5500	30	343	–	–	–
Mb$_{1-99}$	−6600	37	–	415 (415)	3.8	–
apoMb-HAB_F	−8900	39	344	–	–	–
Mb-HAB_F	−12000	48	–	417 (416)	4.4	–
apoMb-B_GHA	−11700	46	344	–	–	–
Mb-B_GHA	−24800	84	–	422 (409)	3.2	no
apoMb-C_GHAB	−12400	48	344	–	–	–
Mb-C_GHAB	−23600	82	–	422 (409)	3.2	no

[a] See Experimental Procedures for details. [b] $\langle\lambda\rangle$ is the center of spectral mass of emission fluorescence calculated as described in eq 1. [c] Numbers outside the parentheses refer to the cyanide form of heme, and numbers inside the parentheses refer to the oxidized form of heme. [d] Does not bind heme (*31*). Errors are less than 4%.

residual molar ellipticity than the WT (Table 1). The WT apoMb had residual molar ellipticity at 222 nm equal to −18000 deg cm^2 dmol^{-1}, whereas Mb$_{1-99}$, Mb-HAB_F, Mb-B_GHA, and Mb-C_GHAB had values of −5500, −8900, −11700, and −12400 deg cm^2 dmol^{-1}, respectively, which means that the calculated helix percentages of the mutants were much lower than the helix percentage of WT (Table 1). Tryptophan fluorescence measurements were used to probe the apoMb tertiary structure, since this protein has two tryptophan residues localized at the A helix (residues 7 and 14), which are buried in the protein tertiary structure at neutral pH (*15*). WT apoMb exhibited an intrinsic emission fluorescence center of mass of ∼338 nm, whereas all mutants had centers of mass of ∼344 nm (Table 1). The value of 344 nm is intermediate between the value of 338 nm for WT and the value of 354 nm measured in the presence of 6 M Gdm-Cl (data not shown), indicating that the tryptophan residues were partially exposed in the mutants. Gel filtration experiments indicated that all mutants in the apo form aggregated at high concentrations (data not shown).

Deleted Mutants Had Non-Native Heme Binding Characteristics and Aggregated. Figure 4A shows the absorbance spectrum profile of the deleted mutants after the heme binding procedure, and Table 1 lists the wavelength of maximum absorption at the Soret region for oxidized and cyano holoproteins. The deletion mutants had a maximum absorption wavelength at 415−417 nm in the absence or presence of cyano (Figure 4A and Table 1). Both holoMb$_{1-99}$ and holoMb-HAB_F had lower molecular ellipticities than WT (Figure 3A), and formed aggregates as shown by gel filtration cromatography (Figure 5A). Binding of heme to Mb-HAB_F had an only partial effect in recovering the secondary structure of the mutant, as shown by its CD profile, while the CD spectra of holoMb$_{1-99}$ had a changed shape without a significant change in its signal at 222 nm (Figure 3A and Table 1).

Permuted Mutants Exhibited Native-like Heme Binding and Were as Well-Folded and Well-Packed as WT. The WT and permutants were mixed with hemin as described in Experimental Procedures and purified by gel filtration chromatography to separate the heme-bound form from the non-heme bound and self-associated forms. Approximately 60% of the WT protein was recovered in the holo form, whereas ∼30% and ∼15% of the Mb-B_GHA and Mb-C_GHAB, respectively, were recovered in the holo form. Figure 4B shows the absorbance spectrum profile of the permuted mutants after the heme binding procedure, and Table 1 lists the wavelength of maximum absorption at the Soret region for oxidized and cyano holoproteins. The WT and circularly permutants had native-like Soret spectra with a maximum absorption wavelength at 408−409 nm when in the oxidized form and at 423 nm when in the cyano form (Figure 4B and Table 1). When heme was bound, permutants and WT proteins had similar ellipticity; the CD signal at 222 nm of Mb-B_GHA and Mb-C_GHAB changed from −11700 and

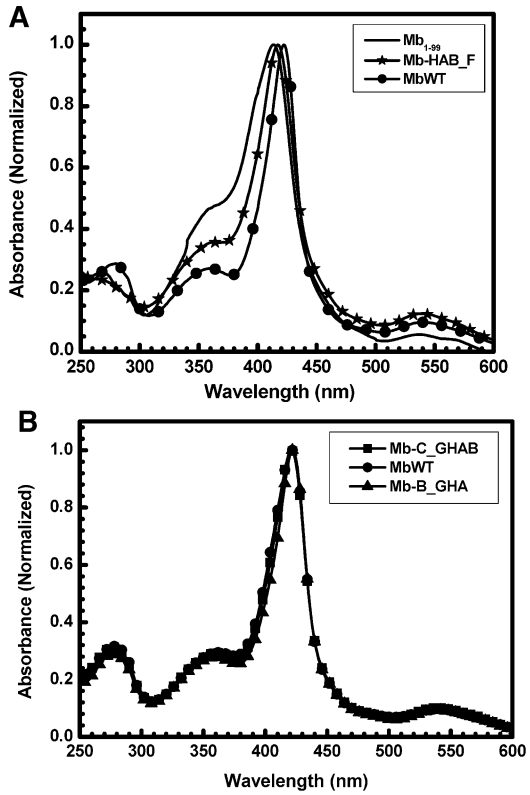

FIGURE 4: Absorption spectra of cyanoMbs. The absorbance spectra at the UV and Soret regions (250−600 nm) were normalized for the sake of comparison. The peak at 280 nm, due to aromatic residues, is shown. (A) WT and deleted mutants. The spectra of the deleted mutants differ from the WT spectrum. (B) WT and circularly permuted mutants. All proteins present absorption peaks at 540, 423, and 360 nm, which are characteristic of a native-like heme coordination. Note that $A_{423}/A_{280} \sim 3.2$ (see the text).

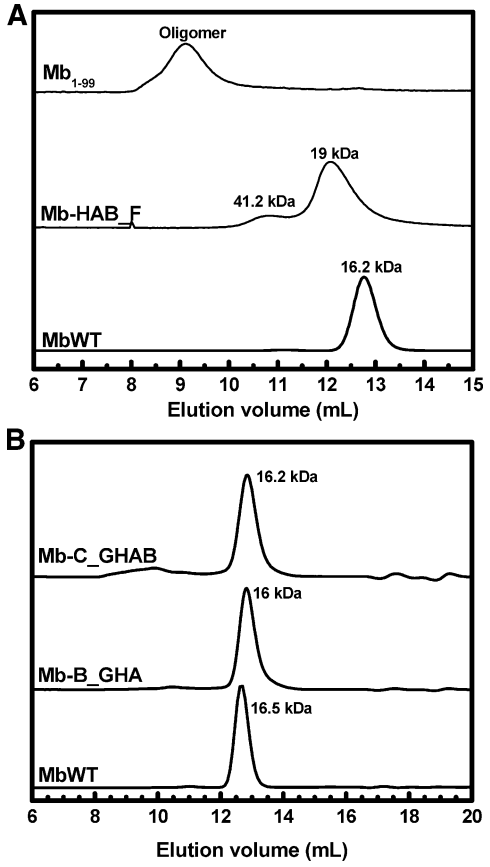

FIGURE 5: Gel filtration chromatography of holoMbs. Protein elution was monitored at A_{280} and A_{423} (Soret band). Only A_{423} values are plotted. All mutants in the apo form exhibited aggregation (data not shown). (A) WT and deleted mutants. The Mb_{1-99} chromatographic profile shows a sole species with a large molecular mass, while the Mb-HAB_F chromatographic profile shows two species. **(**B) WT and circularly permuted mutants. WT and circular permutein chromatography profiles show a sole species with the expected molecular mass.

-12400 deg cm^2 dmol^{-1} for the apo form to -24800 and -23600 deg cm^2 dmol^{-1} for the holo form, respectively (Figure 3B and Table 1). The holopermuteins did not bind bis-ANS (Table 1), a probe that is virtually nonfluorescent in aqueous solution or in the presence of WT holoMb, but becomes fluorescent when bound to partially unfolded structures (*45*), indicating that holopermuteins were as well folded as WT Mb. Sedimentation velocity AUC experiments give information about the shape of the protein being studied. Given the sedimentation coefficient, in conjunction with the molecular mass and partial specific volume, information about the molecular shape in solution can be gained. The sedimentation velocity AUC experiments showed that the holopermuteins had compactness similar to that of WT (Figure 6 and Table 2). The sedimentation coefficients of WT and permuteins were very similar to the sedimentation coefficient of a sphere with the same molecular mass and with a smooth compact shape, indicating that the proteins were compact and well-folded.

Holopermuteins Aggregated and Were Less Stable than WT. Gel filtration experiments showed that the holopermuteins were apparently monomeric at low protein concentrations (<0.5 mg/mL) (Figure 5B), whereas at higher protein concentrations (>0.5 mg/mL), aggregated species were also present (data not shown). Sedimentation velocity AUC is an ideal technique for checking heterogeneity. Figure 6 shows that, at low concentrations, the monomer is the only species found for WT holoMb and was the dominant species found for holopermuteins in solution. However, the holopermuteins presented a small fraction of species with higher sedimentation coefficients, as shown by the presence of a shoulder in their curve profiles (Figure 6). This result confirmed that the permuteins were predisposed to aggregation, a characteristic that restricted the investigations of their structure by NMR. The stabilities of the proteins were investigated by heat-induced unfolding monitored by CD at 222 nm (Figure 7). The proteins were heated to 95 °C and cooled to 20 °C,

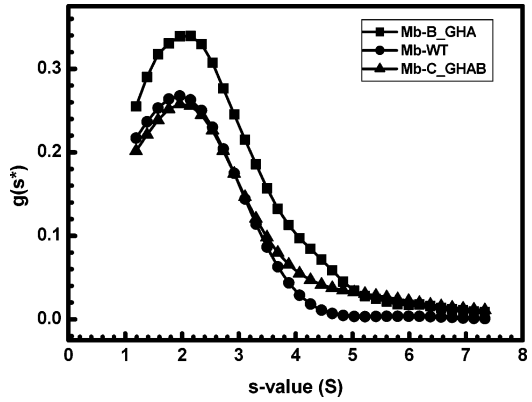

FIGURE 6: Sedimentation velocity UAL of holoMbs. Sedimentation time derivative [$g(s^*)$ integral distribution] analysis of WT and circular permutein velocity sedimentation UAL profiles. The proteins exhibited similar sedimentation coefficients (see Table 2), but holo permuteins have a small fraction of species with higher sedimentation coefficients, which is indicative of aggregation.

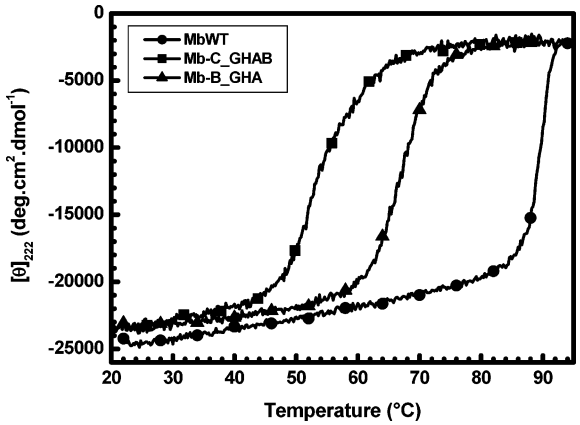

FIGURE 7: Thermally induced unfolding of holoMbs monitored by CD. The differences in stability between the proteins are evident. WT had a T_m, the temperature at the midpoint of the unfolding transition, of 89 °C, whereas Mb-B_GHA had a T_m of 67 °C and Mb-C_GHAB a T_m of 52 °C.

Table 2: Sedimentation Coefficients Measured by Analytical Ultracentrifugation for WT and Permutant HoloMbs[a]

method	WT[b]	Mb-B_GHA[b]	Mb-C_GHAB[b]
$g(s^*)$	2.05	2.09	2.04
second moment	2.04	2.18	2.04
transport	2.05	2.09	2.10
van Holde−Weischet	2.10	2.16	2.10
average	2.06	2.13	2.07
$s_{20,w}$	2.00	2.10	2.05
$s_{sphere,20,w}$	2.11	2.22	2.22

[a] See Experimental Procedures for details. [b] The data are the average of at least three experiments. Errors are less than 2%.

and presented nonreversible unfolding transitions. However, the difference in stability among them was evident; WT had a T_m (temperature at the midpoint of the unfolding transition) of 89 °C, Mb-B_GHA a T_m of 67 °C, and Mb-C_GHAB a T_m of 52 °C.

DISCUSSION

Effects of C-Terminal Helix Deletions. The deletion of C-terminal helices causes destabilization of both the apo and holo forms of Mb. Both the C-terminal, linear, Mb_{1-99}, and Mb_{1-123} (*31*), and circular, Mb-HAB_F, deleted mutants were expressed directly as inclusion bodies, independent of the induction temperature, whereas the WT is expressed as inclusion bodies at 42 °C, but not at 37 °C (*31*). These deleted mutants had both lower stability and weaker ability to bind heme than WT Mb. The apo form of the C-terminal deleted mutants had low α-helical content, had exposed tryptophan residues, and was aggregated. These characteristics appear to be properties of the Mb C-terminal deletion mutations (*30*, *31*). Chow et al. (*30*) studied several Mb mutants with serial C-terminal deletions: helix H deletion [Mb1−119; similar to the Mb_{1-123} mutant (*31*)], FGH deletion (Mb1−77), and CDEFGH deletion (Mb1−36). These mutants aggregate and are β-sheet structured, leading the authors to conclude that apoMb folding is dependent on chain length. The results with the G, H, and GH deleted mutants studied here fit well within the hypothesis of chain length dependence for apoMb folding, reinforcing the importance of nonlocal interactions to the folding of this protein.

Our results add important information that complements other deletion studies of Mb by showing deletion of helix H to be more deleterious, both for the folding and for the heme binding properties, than the deletion of helix G alone or helices G and H. The mutant in which helix G is deleted but helix H is maintained, Mb-HAB_F, and the mutant in which both helices G and H are deleted, Mb_{1-99}, maintained the ability to bind heme and were more stable than the mutant in which only the helix H is deleted, Mb_{1-123} (*31*). Several studies have shown that helix H has a stronger tendency to fold than helix G. Waltho et al. (*46*), studying the secondary structure propensities of apoMb synthetic peptide fragments, showed that helix H is able to form an ordered helix as shown by CD and NMR. However, a peptide corresponding to helix G has a weaker tendency to populate helical conformations (*46*) and is involved in amyloid fibril formation (*47*). These findings are consistent with the study of a fragment corresponding to helices G and H (*48*), which showed that helix H is helical but helix G is unfolded. Several studies showed that helix H is very stable in apoMb, has a significant population of folded helix structure even at pH 2 (*21*, *49*), and is likely to be the first to fold as shown by molecular simulation studies (*50*). Studies of the structure of apoMb by NMR (*20*, *22*) showed that the initial part of helix G is fluctuating. Helix G is well packed against helix H (*19*, *51*), and it may be possible that, in the absence of the latter, the conformational fluctuation of helix G is extended toward its C-terminus, causing a destabilization that is transferred to the whole protein, as seen for Mb_{1-123} (*31*) and Mb1−119 (*30*). As an endorsement of the importance of helix H to the folding of Mb, Mb-HAB_F, which has helix H but not helix G, was more folded than Mb_{1-123}, which has helix G but not helix H.

The C-terminal deleted mutants studied here, Mb-HAB_F and Mb_{1-99}, were able to bind heme, which agrees with the theory of a central core for heme binding exhibited for Mb (*28*, *52*) and also for α and β hemoglobin subunits (*53*). However, the holo forms of the deleted mutants had distorted heme coordination, and heme binding per se was not enough to avoid protein aggregation. HoloMb-HAB_F and $holoMb_{1-99}$ had an altered absorbance spectrum at the Soret band and were not able to show spectral changes in the presence of cyanide. The holo form of these mutants did not show a maximum absorbance peak either at 409 nm (corresponding to the oxidized form) or at 423 nm (corresponding to the cyano form), but it did at 415 nm (both in the presence and in the absence of cyanide), a similar result found for Mb 29−105 (*28*). Among the deleted mutants, only the permuted holoMb-HAB_F had an absorbance peak at 540 nm, considered to be characteristic of specific heme binding (*53*). The low stability and the absence of residues Tyr103, Leu104, Ile107, and Phe138 (Phe138 is present in Mb-HAB_F), which contact the heme group (*54*), may account for the incorrect heme coordination of the deleted mutants studied here. In agreement with these results, the Mb 29−105, which lacks residues Ile107 and Phe138, is expressed as inclusion bodies, has a lower ellipticity than the WT, and shows a maximum absorbance at 415 nm (*28*).

Along with the altered heme coordination discussed above, the deleted mutants were not folded well, and $holoMb_{1-99}$ and holoMb-HAB_F had altered ellipticity and solubility when compared to WT holoMb. The mutants presented highly aggregated species in the gel filtration chromatography profile, and the percentages of α-helices calculated for the deleted mutants were much lower than that of WT, which means that they were less folded. Other results, such as the very poor heme binding ability of $apoMb_{1-123}$ caused by its instability (*31*), and the inability of apoMb mutants without helix A or helices A and B to be even expressed under the conditions described here[2] indicate that apoMb is very unstable in the absence of helices A, B, G, and H and are in accordance with a folding that is dependent on the presence of both the N- and C-termini. Another indication that both N- and C-termini of Mb need to be present for native-like heme binding and folding comes from the poorly structured conformations of the deleted mutants (refs *28*−*31* and this work), in contrast with the well-folded characteristics of the permuted proteins (ref *32* and this work; see below). In conclusion, our results showed that although Mb has a core that is capable of binding heme, helices A, B, G, and H are needed for the correct structural architecture of the protein.

Effects of N-Terminal Circular Permutations. An important question in protein folding is whether the natural N- and C-termini, i.e., the given order of secondary structure segments, is critical for protein folding and stability. The study of circularly permuted proteins may help to answer this question; therefore, we created two circularly permuted Mbs that had the original N-terminus moved to the C-terminus to study the effect of these modifications on folding and stability. The resultant permuteins, Mb-B_GHA and Mb-

[2] E. A. Ribeiro, Jr., and C. H. I. Ramos, unpublished results.

C_GHAB, similar to the deleted mutants, were expressed directly as inclusion bodies independent of the temperature utilized. In the apo form, the permuteins had characteristics of a partially unfolded Mb: low α-helical contents, partially exposed tryptophan residues, and formation of aggregates. These results indicated that these apo permutants were less stable than WT. The measured values for CD at 222 nm and emission fluorescence center of mass for apo permuteins resembled those of the intermediate at pH 4.2 (*15*). The implication of the mutations reported here to the folding pathway of apomyoglobin is under investigation. In this work, we report mainly the findings at neutral pH.

The binding of heme to Mb involves the hydrophobic packing and ligation to His93 in helix F. This binding stabilizes the secondary and tertiary structure of helix F to form the characteristic Mb structure. The holo permuteins had heme binding characteristics similar to those of WT holoMb. Under oxidizing conditions at pH 6.0, the holo permuteins had a maximum absorbance peak at around 409 nm, characteristic of the noncovalent bond between the heme and the two histidines, at positions 93 and 64, which indicated a native-like behavior (*37*). Other indications of native-like heme binding were the shift of the peak position from 409 to ∼423 nm in the presence of cyanide, and the fact that the molar absorbances of the permuteins at 423 nm were ∼3.2 times higher than the molar absorbance at 280 nm, as described for WT Mb (*37*). The other peaks characteristic of a heme correctly bonded to Mb, at 540 and 360 nm, were also present. The observed native-like heme binding of the circularly permuted Mbs can only be explained by a native-like tertiary structure. The low ellipticity measured by far-UV CD is one of the properties that distinguishes apoMb from holoMb (*55*), and heme binding increased the ellipticity of WT Mb from 65 to 85% (Table 1). Heme binding to the permuteins increased their ellipticity from 47 to 83%, which agrees with the proposition that the folding of the heme-binding subdomain of Mb is dependent on the cofactor (heme) (*28*).

The holo permuteins were compact and had native-like folding as shown by gel filtration chromatography, bis-ANS spectroscopy, and AUC experiments. Gel filtration chromatography showed that the holo permutants eluted as proteins with the expected mass for monomer Mbs. WT and permutant holoMbs did not bind bis-ANS, a probe for partially unfolded structures (*45*), showing that they were well-folded. The sedimentation coefficient calculated for WT and permutant holoMbs showed that these proteins had native-like folding and compactness. The correct folding of WT holoMb produced under the conditions described here is confirmed by its NMR spectra (*31*), which increases the confidence that the holo permuteins are indeed well-folded.

The permutations did not cause large changes in the structure of holoMb; however, they caused a large decrease in the stability. A minor fraction of aggregated species can be identified even at low holo permutein concentrations, as shown in the sedimentation velocity AUC experiments, showing that these mutants self-associated. The C-terminal holo permutation unfolds at a much lower urea concentration than WT holoMb (*32*), and the N-terminal holo permutations studied here had a large decrease in the temperature stability that was dependent on the size of the portion that was permuted, and had lower T_m values than even the apo form of WT studied under the same conditions (data not shown). The holo mutant permuted of helix A, Mb-B_GHA, had a T_m ∼22 °C lower than that of WT holoMb, and the holo mutant permuted of helices A and B, Mb-C_GHAB, had a T_m ∼37 °C lower than that of WT holoMb. After incubation for 2 days at 37 °C, the holo permuteins aggregated (flocculation identified even by the naked eye), whereas WT holoMb remained soluble for weeks (data not shown). The much lower stability of the holo permuteins compared to WT holoMb indicates that they would be unfolded and aggregated inside the cell under physiological conditions. The aggregation of a protein inside the cell is very dangerous, particularly in the case of Mb, which is present at high concentrations and can form amyloid fibrils (*56*−*58*). Likewise, aggregation will be worsened in the case of these permutations since they maintained this characteristic even when heme was bound, while heme binding appears to abolish the aggregation of the WT protein (*47*).

Implications for Myoglobin Folding. This work provides further evidence that helices A, G, and H work as nuclei for Mb folding and stability, which agrees with several recent lines of evidence that point to this conclusion. ApoMb unfolded at pH 2.3 exhibits some long-range contacts between residues in helices G and H and between residues in helix A and helices G and H that are typical of the native state (*49*). Molecular dynamics experiments showing that interactions between helices A and H are the last to be lost in unfolding simulations (*50*) corroborate the hypothesis that structures in these two helices are among the first to be formed. Chow et al. (*30*) suggested that the N-terminus of apoMb becomes progressively enriched in α-helical content as the chain elongates, being completely folded only when helix H is present. Ptitysin and Ting (*59*) used an empirical phylogenetic method to show that important positions for the folding of globins are found in helices A, G, and H. This evidence and our results showing that the deletion of helix H is more deleterious than the deletion of helix G agree with a model in which helix H is necessary for the proper folding of helix G and therefore acts as a nucleus for Mb folding. The absence of helix G, even when helix H is present (mutant Mb-HAB_F), also affected the proper folding of Mb, showing that this helix is important for the stability of the other helices in Mb. The fact that mutants lacking helix A were not expressed under the conditions described here indicates that helix A also serves as a nucleus to the Mb folding. Thus, the deletion of helix A, G, or H, as shown here, causes severe problems in the proper Mb folding, and deletion of all of them results in an unfolded protein (*28*).

The formation of helices A, G, and H in the intermediate with the subsequent combination of the partially folded B helix (the A[B]GH core) is confirmed by NMR studies (*21*, *23*, *24*), and is considered to be an important step in apoMb reaching its native state (*15*, *26*, *27*). The two permutants studied here covalently put together either GHA or GHAB segments, and therefore, they differ in the position of helix B. In Mb-B_GHA, helix B is away from the GHA domain, whereas in Mb-C_GHAB, this helix is covalently attached to the GHA domain. Further studies of these permuteins at pH 4 are underway, and they may help to understand the structure of helix B in the intermediate. Nonetheless, these apo permuteins were not as folded as the WT, and their ellipticity resembled that of the WT intermediate. Since it is

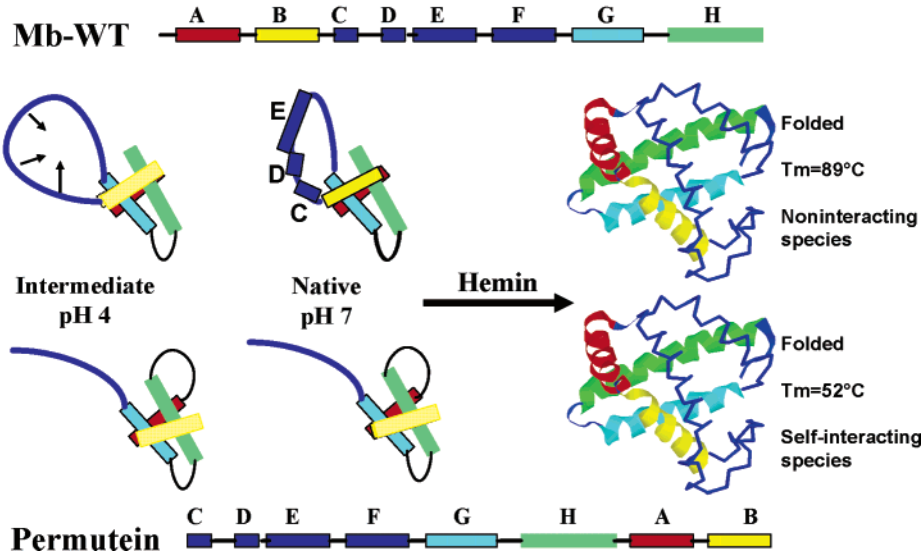

FIGURE 8: Schematic diagram illustrating the events occurring with WT and permuteins upon folding and heme binding. A box represents a folded or partially folded helix and a line an unfolded helix. The dots in helix B indicate the uncertainty in the extension of its folding in the intermediate. See the text for a discussion.

well established that the formation of the A[B]GH core at pH 4 is due to its higher helix propensity compared to that of the CDEF subdomain (*60*), and that the fragment comprising residues 29−105 has poor α-helical structure (*28*), we suggest that the permuteins studied here have a well-formed A[B]GH core but have either an unfolded or a partially folded CDEF subdomain when they are in the apo form. This hypothesis implies that the establishment of the A[B]GH core, formed by N- and C-terminal segments, is important for constraining the conformational freedom of the central portion of apoMb, facilitating its folding (Figure 8). In the permuteins, the formation of the A[B]GH core did not constrain the conformational space of the CDEF subdomain, which then did not realize proper folding, resulting in permuteins with CD and fluorescence characteristics of the pH 4 intermediate at neutral pH (in fact, the CD spectra of the permuteins did not change from pH 7 to 4; data not shown). In WT apoMb, sequential heme binding causes folding of the E−F loop, helix F, the F−G loop, and the beginning of helix G, increasing the compactness of the protein (*21*). In the permutants, heme binding appears to cause the folding of the entire CDEF subdomain as expected from results with the Mb 29−105, in which CD spectrum changes from a random coil profile to an α-helical profile upon addition of hemin (see Figure 4 in ref *28*). In conclusion, our data are compatible with a model for Mb folding in which the formation of the A[B]GH core helps to constrain the polypeptide backbone fluctuations in the CDEF subdomain. With both N- and C-termini constrained in the core, the central portion, i.e., the CDEF subdomain, has restricted conformational space, helping its folding. In the apo permutants, the CDEF subdomain is not constrained by the formation of the A[B]-GH core and remains unfolded or only partially folded until heme binding provokes its folding (Figure 8).

Although the holo permuteins remain as folded and compact as the WT Mb, they had lower stability and had a tendency to aggregate, indicating that the correct position of the N-terminus is important for protein stability. Other proteins exhibit the same behavior. For instance, the recombinant α-lactalbumin has an extra methionine residue in its N-terminus for *Escherichia coli* expression purposes, causing a strong destabilization of the protein, although the overall structures of the authentic and recombinant proteins remain the same (*61*). It seems that the alterations at the N-terminus did not cause large changes in the tertiary structure of a protein; however, these changes may have at least subtle effects on the general stability. In conclusion, the correct position of myoglobin N- and C-termini appears not to be required for the native folding in the presence of heme, and for the native-like heme pocket formation; however, it is required for Mb stability and solubility. Since the circular permutations were less stable and showed fibril-like characteristics, we concluded that myoglobin N- and C-termini have to be native-like for the correct structural architecture of this protein. These results are consistent with the Anfinsen hypothesis (*14*), which states that the amino acid sequence determines the conformation with higher stability.

ACKNOWLEDGMENT

We thank the referees for their helpful suggestions and Drs. M. Santoro, S. T. Ferreira, and M. Jamin for helpful discussions. We thank Dr. C. Benedetti for critical reading of this manuscript and V. Soares, L. Rodrigues, and S. Silva for technical assistance. The idea to create the pT7-7-2MB clone was originated in a discussion with Dr. M. Kay.

REFERENCES

1. Chotia, C. (1984) Principles that determine the structure of proteins, *Annu. Rev. Biochem. 53*, 537−572.
2. Woolfson, D. N., Evans, P. A., Hutchinson, E. G., and Thornton, J. M. (1993) Topological and stereochemical restrictions in *β*-sandwich protein structures, *Protein Eng. 6*, 461−470.
3. Pan, T., and Uhlenbeck, O. C. (1993) Circularly permuted DNA, RNA and proteins: A review, *Gene 125*, 111−114.
4. Heinemann, U., and Hahn, M. (1995) Circular permutation of polypeptide chains: Implications for protein folding and stability, *Prog. Biophys. Mol. Biol. 64*, 121−143.
5. Jaenicke, R. (1999) Stability and folding of domain proteins, *Prog. Biophys. Mol. Biol. 71*, 155−241.
6. Ramos, C. H. I., and Ferreira, S. T. (2005) Protein folding, misfolding and aggregation: Evolving concepts and conformational diseases, *Protein Pept. Lett. 12*, 213−222.

7. Goldenberg, D. P., and Creighton, T. E. (1983) Circular and circularly permuted forms of bovine pancreatic trypsin inhibitor, *J. Mol. Biol. 165*, 407−413.
8. Luger, K., Hommel, U., Herold, M., Hofsteenge, J., and Kirschner, K. (1989) Correct folding of circularly permuted variants of a $\beta\alpha$ barrel enzyme in vivo, *Science 243*, 206−210.
9. Zhang, T., Bertelsen, E., Benvegnu, D., and Alber, T. (1993) Circular permutation of T4 lysozyme, *Biochemistry 32*, 12311−12318.
10. de Prat Gay, G., Ruiz-Sanz, J., Neira, J. L., Corrales, F. J., Otzen, D. E., Ladurner, A. G., and Fersht, A. R. (1995) Conformational pathway of the polypeptide chain of chymotrypsin inhibitor-2 growing from its N terminus in vitro. Parallels with the protein folding pathway, *J. Mol. Biol. 254*, 968−979.
11. Viguera, A. R., Blanco, F. J., and Serrano, L. (1995) The order of secondary structure elements does not determine the structure of a protein but does affect its folding kinetics, *J. Mol. Biol. 247*, 670−681.
12. Ramos, C. H. I. (1999) Mapping subdomains in the C-terminal region of troponin I involved in the binding to troponin C and to thin filament, *J. Biol. Chem. 274*, 18189−18195; (2000) *J. Biol. Chem. 275*, 6045 (Erratum).
13. Smith, V. F., and Matthews, C. R. (2001) Testing the role of chain connectivity on the stability and structure of dihydrofolate reductase from *E. coli*: Fragment complementation and circular permutation reveal stable, alternatively folded forms, *Protein Sci. 10*, 116−128.
14. Anfinsen, C. B., Haber, E., Sela, M., and White, F. H., Jr. (1961) The kinetics of formation of native ribonuclease during oxidation of the reduced polypeptide chain, *Proc. Natl. Acad. Sci. U.S.A. 47*, 1309−1314.
15. Wright, P. E., and Baldwin, R. L. (2000) Case study 1: The folding of apomyoglobin, *Mechanisms of protein folding*, 2nd ed., pp 309−329, Oxford University Press, New York.
16. Brunori, M. (2000) Structural dynamics of myoglobin, *Biophys. Chem. 86*, 221−230.
17. Wittenberg, J. B., and Wittenberg, B. A. (2003) Myoglobin function reassessed, *J. Exp. Biol. 206*, 2011−2020.
18. Jamin, M. (2005) The folding process of apomyoglobin, *Protein Pept. Lett. 12*, 229−234.
19. Takano, T. (1977) Structure of myoglobin refined at 2.0 Å resolution I. Crystallographic refinement of metmyoglobin from sperm whale, *J. Mol. Biol. 110*, 537−568.
20. Eliezer, D., and Wright, P. E. (1996) Is apomyoglobin a molten globule? Structural characterization by NMR, *J. Mol. Biol. 263*, 531−538.
21. Eliezer, D., Yao, J., Dyson, H. J., and Wright, P. E. (1998) Structural and dynamic characterization of partially folded states of apomyoglobin and implications for protein folding, *Nat. Struct. Biol. 5*, 148−155.
22. Lecomte, J. T., Sukits, S. F., Bhattacharya, S., and Falzone, C. J. (1999) Conformational properties of native sperm whale apomyoglobin in solution, *Protein Sci. 8*, 1484−1491.
23. Hughson, F. M., Wright, P. E., and Baldwin, R. L. (1990) Structural characterization of a partly folded apomyoglobin intermediate, *Science 249*, 1544−1548.
24. Jennings, P. A., and Wright, P. E. (1993) Formation of a molten globule intermediate early in the kinetic folding pathway of apomyoglobin, *Science 262*, 892−896.
25. Jamim, M., and Baldwin, R. L. (1998) Two forms of the pH 4 folding intermediate of apomyoglobin, *J. Mol. Biol. 276*, 491−504.
26. Loh, S. N., Kay, M. S., and Baldwin, R. L. (1995) Structure and stability of a second molten globule state intermediate in the apomyoglobin folding pathway, *Proc. Natl. Acad. Sci. U.S.A. 92*, 5446−5450.
27. Kiefhaber, T., and Baldwin, R. L. (1995) Intrinsic stability of individual α-helices modulates structure and stability of the apomyoglobin molten globule form, *J. Mol. Biol. 252*, 122−132.
28. Grandori, R., Schwarzinger, S., and Müller, N. (2000) Cloning, overexpression and characterization of micro-myoglobin, a minimal heme-binding fragment, *Eur. J. Biochem. 267*, 1168−1172.
29. De Sanctis, G., Ascoli, F., and Brunori, M. (1994) Folding of apominimyoglobin, *Proc. Natl. Acad. Sci. U.S.A. 91*, 11507−11511.
30. Chow, C. C., Chow, C., Raghunathan, V., Huppert, T. J., Kimball, E. B., and Cavagnero, S. (2003) Chain length dependence of apomyoglobin folding: Structural evolution from misfolded sheets to native helices, *Biochemistry 42*, 7090−7099.
31. Ribeiro-Júnior, E. A., Regis, W. C. B., Tasic, L., and Ramos, C. H. I. (2003) Fast purification of the apo form and of a non-binding heme mutant of recombinant sperm whale myoglobin, *Protein Expression Purif. 28*, 202−208.
32. Fishburn, A. L., Keeffe, J. R., Lissounov, A. V., Peyton, D. H., and Anthony-Cahill, S. J. (2002) A circularly permuted myoglobin possesses a folded structure and ligand binding similar to those of the wild-type protein but with a reduced thermodynamic stability, *Biochemistry 41*, 13318−13327.
33. Ribeiro, E. A., Jr., and Ramos, C. H. I. (2004) Origin of the anomalous circular dichroism spectra of many apomyoglobin mutants, *Anal. Biochem. 329*, 300−306.
34. Edelhoch, H. (1967) Spectroscopic determination of tryptophan and tyrosine in proteins, *Biochemistry 6*, 1948−1954.
35. Ramos, C. H. I. (2004) A Spectroscopic-based Laboratory Course for Protein Conformational Studies, *Biochem. Mol. Biol. Educ. 32*, 31−34.
36. Ramos, C. H. I., Kay, M. S., and Baldwin, R. L. (1999) Putative ion pairs involved in myoglobin stability, *Biochemistry 38*, 9783−9790.
37. Antonini, E., and Brunori, M. (1971) *Hemoglobin and Myoglobin in Their Reactions with Ligands*, American Elsevier Publishing Co., New York.
38. Chen, Y. H., Yang, J. T., and Chau, K. H. (1974) Determination of the helix and b-form of proteins in aqueous solution by circular dichroism, *Biochemistry 13*, 3350−3359.
39. Schuck, P. (2000) Size distribution analysis of macromolecules by sedimentation velocity ultracentrifugation and Lamm equation modeling, *Biophys. J. 78*, 1606−1619.
40. van Holde, K. E., and Wolfgang, O. (1978) Weischet boundary analysis of sedimentation-velocity experiments with monodisperse and paucidisperse solutes, *Biopolymers 17*, 1387−1403.
41. Goldberg, R. J. (1953) Sedimentation in the ultracentrifuge, *J. Phys. Chem. 57*, 194−202.
42. Baldwin, R. L. (1953) Sedimentation coefficients of small molecules: Methods of measurement based on the refractive-index gradient curve. The sedimentation coefficient of polyglucose A, *Biochem. J. 55*, 644−648.
43. Stafford, W. F. (1994) Boundary analysis in sedimentation velocity experiments, *Methods Enzymol. 240*, 478−501.
44. Lebowitz, J., Lewis, M. S., and Schuck, P. (2002) Modern analytical ultracentrifugation in protein science: A tutorial review, *Protein Sci. 11*, 2067−2079.
45. Stryer, L. (1965) The interaction of a naphthalene dye with apomyoglobin and apohemoglobin. A fluorescent probe of nonpolar binding sites, *J. Mol. Biol. 13*, 482−495.
46. Waltho, J. P., Feher, V. A., Merutka, G., Dyson, H. J., and Wright, P. E. (1993) Peptide models of protein folding initiation sites. 1. Secondary structure formation by peptides corresponding to the G- and H-helices in myoglobin, *Biochemistry 32*, 6337−6347.
47. Fandrich, M., Forge, V., Buder, K., Kittler, M., Dobson, C. M., and Diekmann, S. (2003) Myoglobin forms amyloid fibrils by association of unfolded polypeptide segments, *Proc. Natl. Acad. Sci. U.S.A. 100*, 15463−15468.
48. Shin, H. C., Merutka, G., Waltho, J. P., Tennant, L. L., Dyson, H. J., and Wright, P. E. (1993) Peptide models of protein folding initiation sites. 3. The G−H helical hairpin of myoglobin, *Biochemistry 32*, 6356−6364.
49. Lietzow, M. A., Jamin, M., Jane Dyson, H. J., and Wright, P. E. (2002) Mapping long-range contacts in ahighly unfolded protein, *J. Mol. Biol. 322*, 655−662.
50. Onufriev, A., Case, D. A., and Bashford, D. (2003) Structural details, pathways, and energetics of unfolding apomyoglobin, *J. Mol. Biol. 325*, 555−567.
51. Kay, M. S., Ramos, C. H. I., and Baldwin, R. L. (1999) Specificity of native-like interhelical hydrophobic contacts in the apomyoglobin intermediate, *Proc. Natl. Acad. Sci. U.S.A. 96*, 2007−2012.
52. De Sanctis, G., Falcioni, G., Giardina, B., Ascoli, F., and Brunori, M. (1988) Mini-myoglobin. The structural significance of haem-ligand interactions, *J. Mol. Biol. 200*, 725−733.
53. Craik, C. S., Buchman, S. R., and Beychok, S. (1980) Characterization of globin domains: Heme bindinig to the central exon product, *Proc. Natl. Acad. Sci. U.S.A. 77*, 1384−1388.
54. Hargrove, M. S., Wilkinson, A. J., and Olson, J. S. (1996) Structural factors governing hemin dissociation from metmyoglobin, *Biochemistry 35*, 11300−11305.
55. Breslow, E., Beychok, S., Hardman, K. D., and Gurd, F. R. N. (1965) Relative conformations of sperm whale metmyoglobin and apomyoglobin in solution, *J. Biol. Chem. 240*, 304−309.
56. Fandrich, M., Fletcher, M. A., and Dobson, C. M. (2001) Amyloid fibrils from muscle myoglobin, *Nature 410*, 165−166.

57. Sirangelo, I., Malmo, C., Casillo, M., Mezzogiorno, A., Papa, M., and Irace, G. (2002) Tryptophanyl substitutions in apomyoglobin determine protein aggregation and amyloid-like fibril formation at physiological pH, *J. Biol. Chem. 277*, 45887−45891.
58. Sirangelo, I., Malmo, C., Iannuzzi, C., Mezzogiorno, A., Bianco, M. R., Papa, M., and Irace, G. (2004) Fibrillogenesis and cytotoxic activity of the amyloid-forming apomyoglobin mutant W7FW14F, *J. Biol. Chem. 279*, 13183−13189.
59. Ptitsyn, O. B., and Ting, K. L. (1999) Non-functional conserved residues in globins and their possible role as a folding nucleus, *J. Mol. Biol. 291*, 671−682.
60. Reymond, M. T., Merutka, G., Dyson, H. J., and Wright, P. E. (1997) Folding propensities of peptide fragments of myoglobin, *Protein Sci. 6*, 706−716.
61. Chaudhuri, T. K., Horii, K., Yoda, T., Arai, M., Nagata, S., Terada, T. P., Uchiyama, H., Ikura, T., Tsumoto, K., Kataoka, H., Matsushima, M., Kuwajima, K., and Kumagai, I. (1999) Effect of the extra N-terminal methionine residue on the stability and folding of recombinant α-lactalbumin expressed in *Escherichia coli*, *J. Mol. Biol. 285*, 1179−1194.

BI047908C